Supporting Information

Fluorescent Janus Emulsions for Biosensing of Listeria Monocytogenes

*Jie Li, Suchol Savagatrup, Zachary Nelson, Kosuke Yoshinaga, Timothy M. Swager**

Department of Chemistry and Institute for Soldier Nanotechnologies, Massachusetts Institute of Technology, Cambridge, MA 02139, USA

Table of Contents

www.pnas.org/cgi/doi/10.1073/pnas.2002623117

Figure S28. Optical images taken by smartphone of non-agglutinated or agglutinated droplets (low magnification)

Figure S29. Images of Janus droplets on top of the waveguide device taken without or with the addition of Listeria

Instruments

NMR spectra were recorded with a Bruker Ascend-400 (400 MHz), JEOL model JNM-ECZ500R/S1 (500 MHz), or Ascend-600 (600 MHz) spectrometer. Chemical shifts δ are reported in ppm downfield from tetramethylsilane using the residual solvent signals ($CDCl_3$: δ_H 7.26 ppm, δ_C 77.16 ppm; acetone-d_6: δ_H 2.05 ppm, δ_C 206.26 ppm) as an internal reference. For ^1H NMR, coupling constants J are given in Hz and the resonance multiplicity is described as s (singlet), d (doublet), t (triplet), p (quintet), and m (multiplet). Mass spectra were recorded with a high-resolution JEOL AccuTOF 4G LC-plus equipped with an ionSense DART source, and a Bruker Autoflex Speed MALDI-TOF (Matrix-Assisted Laser Desorption/Ionization Time-of-Flight Mass Spectrometer) in Reflectron Detection mode, or a JEOL AccuTOF 4G with an IonSense DART (Direct Analysis in Real Time) source. Mass spectra were calibrated using either poly(ethylene glycol) of the appropriate mass range as external standards, or reserpine as an internal standard. UV-Vis absorbance spectra were recorded on a Cary 4000 UV-Vis spectrophotometer using a quartz cuvette. Fluorescence spectra were obtained at room temperature using a bifurcated fiber on a Horiba Jobin Yvon SPEX Fluorolog-τ3 fluorimeter (model FL-321, 450 W Xenon lamp).

Image Analysis

The areas covered by the agglutination of the Janus droplets were calculated by the image analysis. The in-house MATLAB program evaluates the optical intensity within the image and assigns areas with agglutinated droplets. Specifically, the program uses an adaptive thresholding algorithm to distinguish regions of agglutinated droplets (darker areas with opaque regions) from those of pristine droplets (higher transparency, brighter areas). The agglutination % is then calculated by taking the ratio between the agglutinated area and the total area. We note that in some of our images for the control concentration (0 CFU mL^{-1}), the program calculated a non-zero agglutination %. We attributed this error to the abnormally dark regions (*e.g.*, impurity and dust particles) that led to the mistakes in the thresholding step of the program. However, the absolute values for the control samples were small; and, for each concentration of the HKLM, we observed no overlapping in the average value and the standard deviation of the agglutination %.

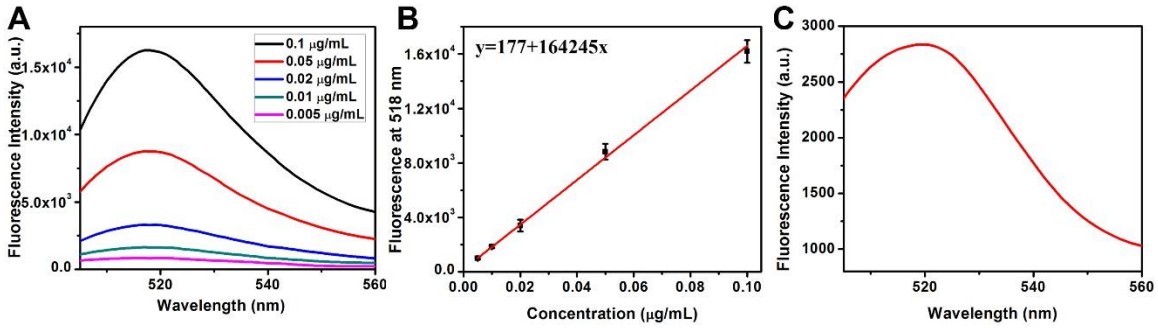

Figure S1. (A) Fluorescence emission spectra (λ_{ex} = 490nm) of known amounts of Protein A-FITC; (B) calibration curve (emission measured at 518 nm); (C) fluorescence emission spectra (λ_{ex} = 490 nm) of re-dissolved dried droplets.

Experimental Procedure for Synthesis of Sub-Phthalocyanine

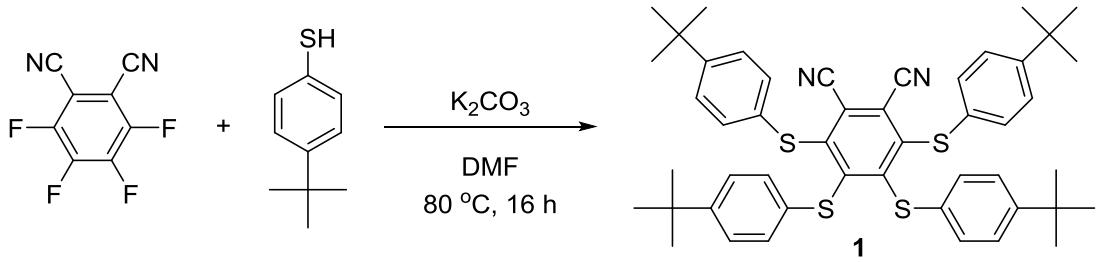

3,4,5,6-tetrakis((4-(*tert*-butyl)phenyl)thio)phthalonitrile (1)

Procedure adapted from reference 1. To a 250 mL Schlenk flask with a stirrer containing 3,4,5-tetrafluorophthalonitrile (2.0 g, 10 mmol) under argon was added dry DMF (100 mL), 4-(*tert*-butyl)benzenethiol (7.1 mL, 41 mmol). Then K_2CO_3 (8.3 g, 60 mmol) was added under a flow of argon. The reaction was stirred at 80 °C for 16 hours. The reaction mixture was cooled to room temperature and diluted with water and chloroform. The layers were separated, and the aqueous layer was extracted twice with chloroform. The combined organic layers were washed four times with water and once with brine, dried over Mg_2SO_4, and filtered. The filtrate was concentrated under reduced pressure and purified by recrystallization from hot acetonitrile to yield an orange powder (6.3 g, 81%). **^{1}H NMR** (400 MHz, Chloroform-d) δ 7.29 (d, J = 8.1 Hz, 4H), 7.25 (d, J = 8.3f Hz, 4H), 7.13 (d, J = 8.2 Hz, 4H), 6.95 (d, J = 8.1 Hz, 4H), 1.29 (d, J = 2.7 Hz, 36H). **^{13}C NMR** (101 MHz, Chloroform-d) δ 152.65, 151.78, 150.99, 146.16, 132.57, 131.13, 130.70, 129.68, 126.70, 126.57, 123.03, 113.96, 34.81, 34.75, 31.37, 31.33. **HRMS** m/z calculated for $C_{48}H_{53}N_2S_2$ $[M+H]^+$: 785.3092, found 785.3079.

Subphthalocyanine (2)

Procedure adapted from reference 2. BCl_3 (1.0 mL, 1 M solution in *p*-xylene) was added to phthalonitrile **1 (**785 mg, 1 mmol) and stirrer under argon in a 25 mL two-necked round-bottomed flask fitted with a condenser and septum. The septum was replaced with a glass stopper, and the apparatus was placed in a pre-heated oil bath at 160 °C and stirred for 30 minutes. After cooling

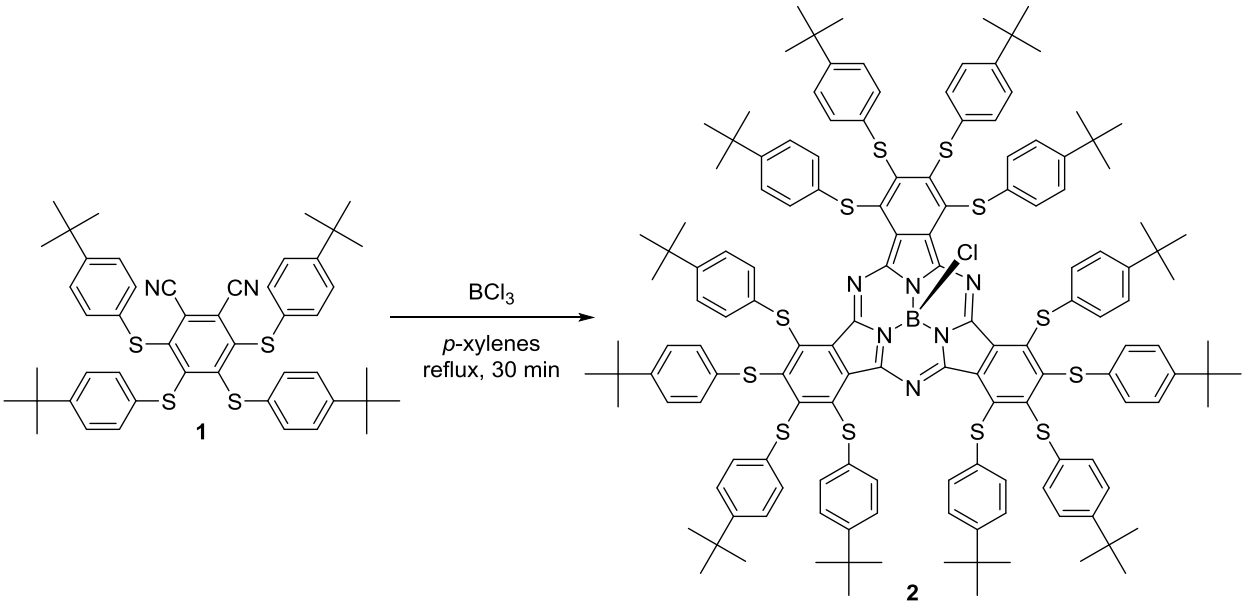

to room temperature, the solution was concentrated under reduced pressure. The resulting blue solid was subjected to silica gel column chromatography with toluene/hexanes (2:3, v:v) as eluent, yielding **2** as a dark blue solid (62 mg, 8%). **^{1}H NMR** (600 MHz, Chloroform-d) δ 7.32 (d, J = 8.7 Hz, 12H), 7.11 (d, J = 8.7 Hz, 12H), 7.06 (d, J = 8.7 Hz, 12H), 6.92 (d, J = 8.7 Hz, 12H), 1.21 (s, 54H), 1.15 (s, 54H). **^{13}C NMR** (151 MHz, Chloroform-d) δ 149.45, 149.36, 149.31, 147.73, 139.80, 134.72, 134.60, 133.69, 129.42, 128.63, 125.95, 125.92, 34.54, 34.49, 31.42, 31.35. **MALDI-TOF** m/z calculated for $C_{144}H_{156}BClN_6S_{12}$ $[M]^+$: 2397.886, found 2397.920. **UV/Vis** (Toluene): λ_{max} (log ε) =310 (11.0), 645 (11.3).

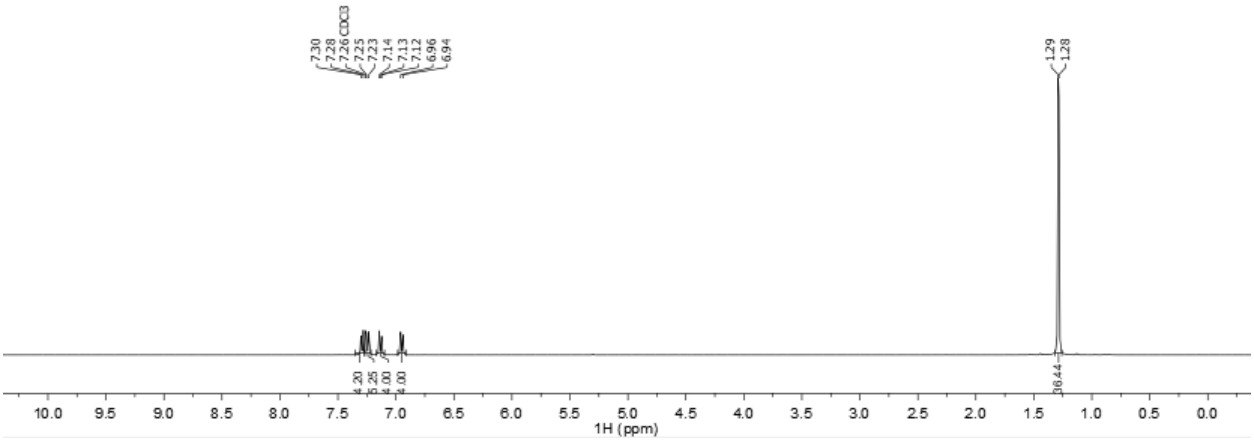

Figure S2. ^{1}H NMR spectrum (400 MHz, Chloroform-d) of **3,4,5,6-tetrakis((4-(tert-butyl)phenyl)thio)phthalonitrile (1)**.

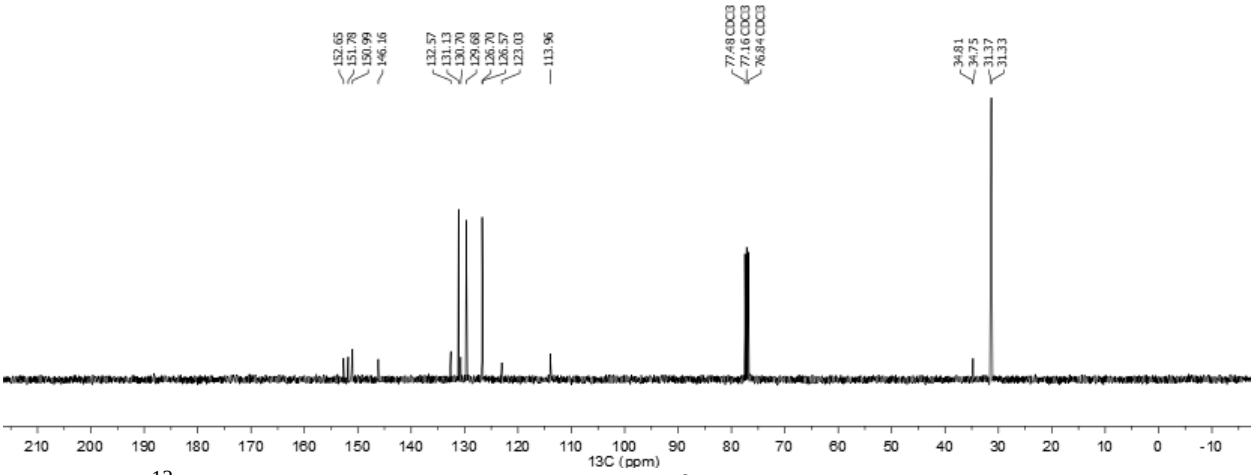

Figure S3. ^{13}C NMR spectrum (101 MHz, $CDCl_3$) of **3,4,5,6-tetrakis((4-(tert-butyl)phenyl)thio)phthalonitrile (1)**.

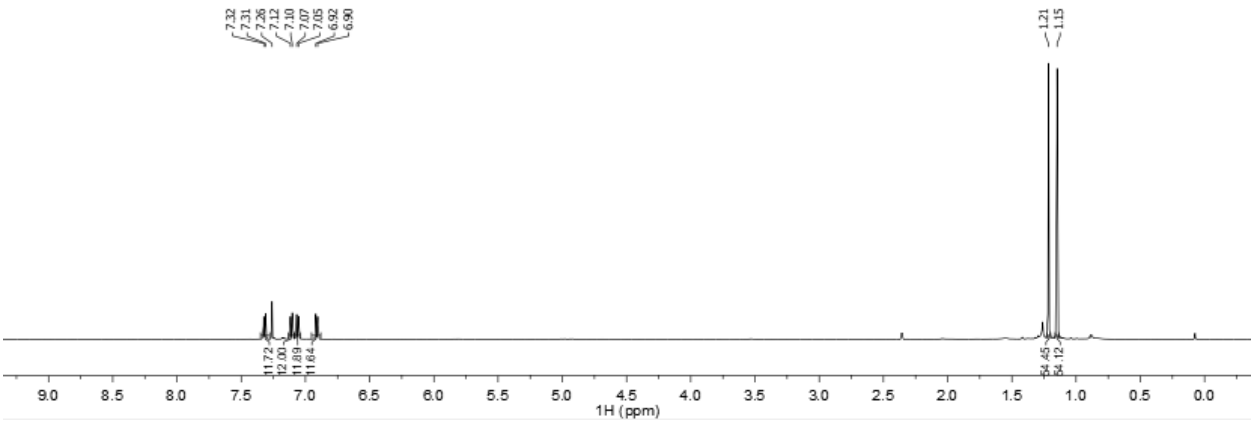

Figure S4. ^{1}H NMR spectrum (600 MHz, Chloroform-d) of **Subphthalocyanine (2).**

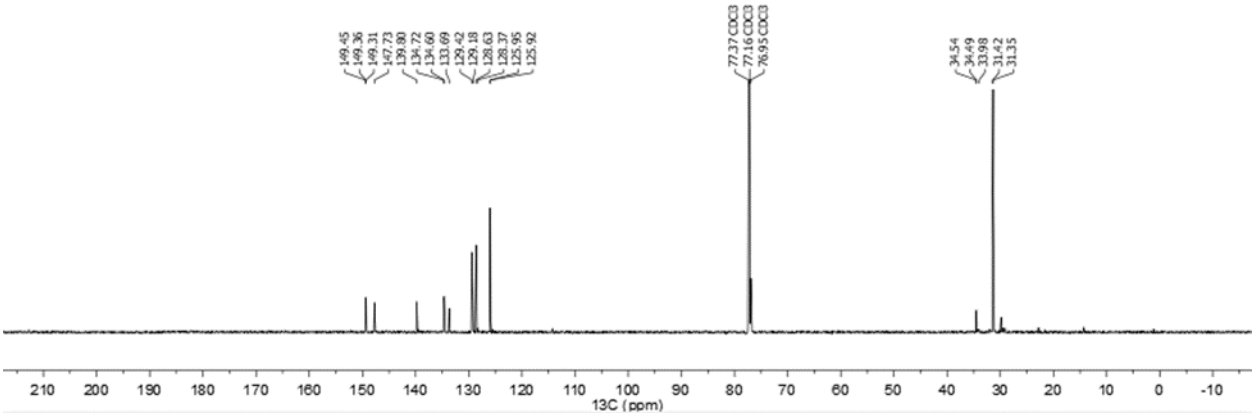

Figure S5. ^{13}C NMR spectrum (151 MHz, Chloroform-d) of **Subphthalocyanine (2).**

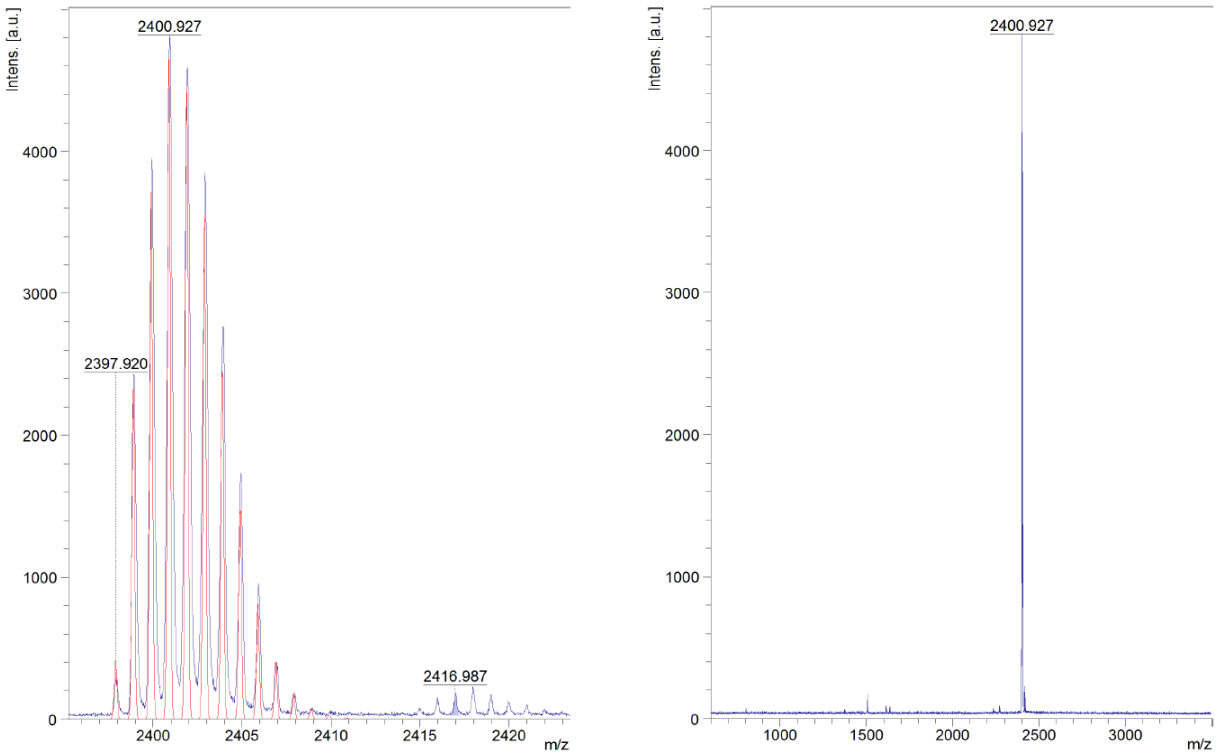

Figure S6. MALDI-TOF mass spectrometry spectrum of **subphthalocyanine (2)** shown in blue. Simulated isotopic distribution for $C_{144}H_{156}BClN_6S_{12}$ shown in red.

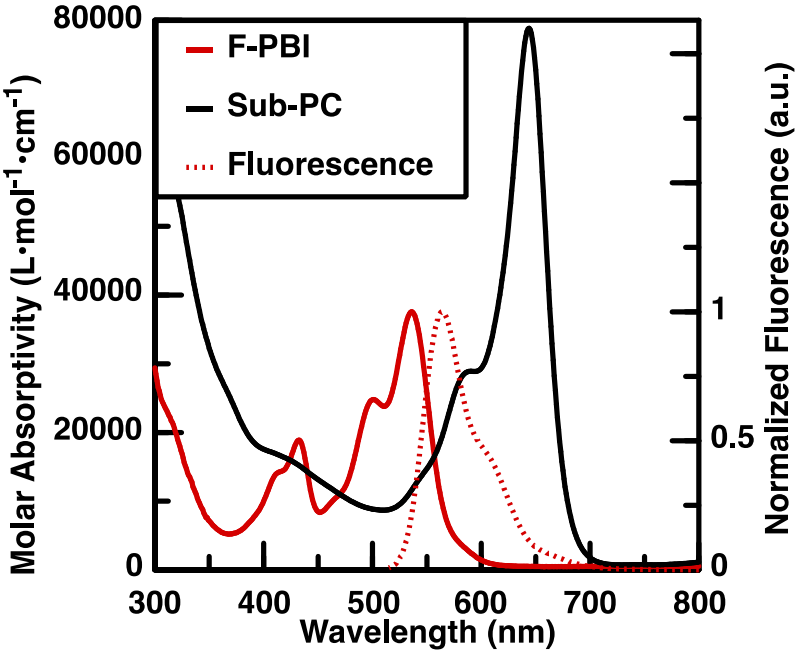

Figure S7. UV/Vis spectra of **subphthalocyanine (2)** in diethylbenzene and **F-PBI** in HFE7500, overlayed with fluorescence specrum of **F-PBI** in HFE7500.

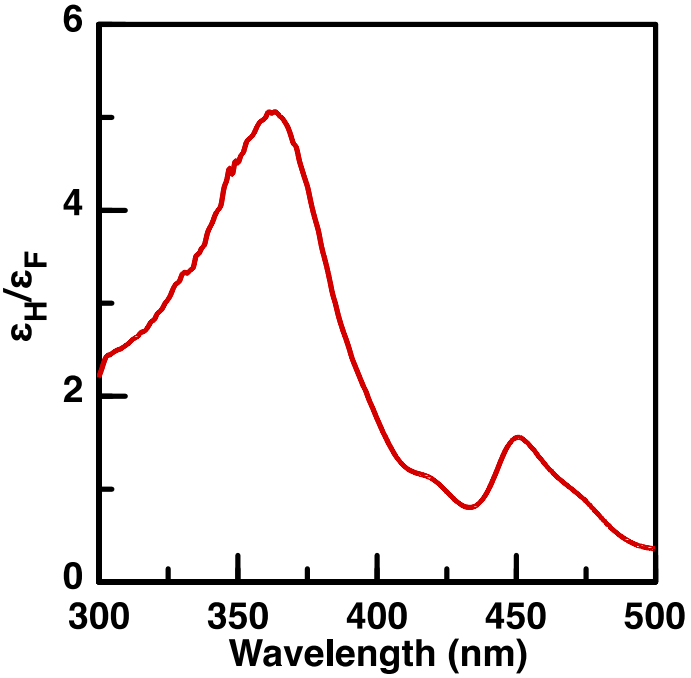

Figure S8. Ratio of molar absorptivity of **subphthalocyanine (2)** (ε_H) and **F-PBI** (ε_F).

Experimental Procedure for Synthesis of F-sub-PC

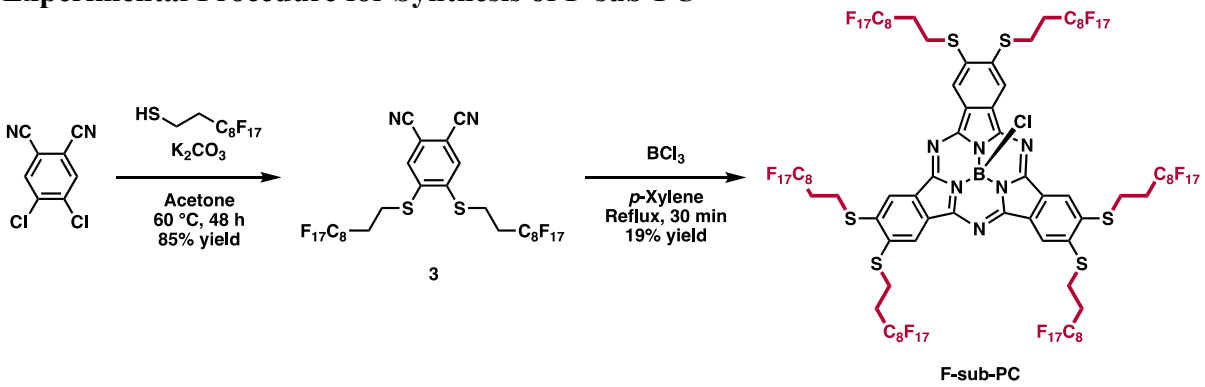

Synthesis of Compound 3. A mixture of 4,5-dichlorophthalonitrile (98.5 mg, 0.500 mmol), 1*H*,1*H*,2*H*,2*H*-perfluorodecanethiol (504 mg, 1.05 mmol), and anhydrous K_2CO_3 (400 mg, 2.89 mmol) in acetone (5 mL) was stirred at 60 °C for 48 h. Then, 1M HCl aq (10 mL) was added and the product precipitated. The precipitate was filtered and collected, and was recrystallized from chloroform to provide colorless crystals **3** (462 mg, 0.426 mmol, 85% yield). **^{1}H NMR** (500 MHz, acetone-d_6, 25 °C): δ (ppm) 8.06 (s, 2H), 3.59 (t, J = 7.6 Hz, 4H), 2.68-2.84 (m, 4H). **^{13}C NMR** (126 MHz, acetone-d_6, 25 °C): δ (ppm) 143.70, 131.54, 116.43, 113.43, 31.10 (t, J = 22 Hz), 24.35. **^{19}F NMR** (471 MHz, acetone-d_6, 25 °C): δ (ppm) -81.56 (t, J = 9.8 Hz, 6F), -114.23 (m, 4F), -122.14 (m, 4F), -122.37 (m, 8F), -123.19 (m, 4F), -123.67 (m, 4F), -126.66 (m, 4F). **DART MS**: m/z calcd. for $C_{28}H_{10}F_{34}N_2S_2$ $[M]^+$: 1083.9742, found: 1083.9742.

Synthesis of F-sub-PC. Compound **3** (462 mg, 0.426 mmol) was added to a dried flask, and BCl_3 (1.0 M in *p*-xylene, 0.450 mL) was added dropwisely. Then, the reaction mixture was stirred at 160 °C in a pre-heated oil bath for 30 min. Upon cooling the reaction mixture to room temperature, it was diluted with FC-770 (5 mL) and transferred to a separation funnel. The fluorous layer was washed with chloroform (10 mL), acetone (10 mL), water, (10 mL), brine (10 mL), dried with $MgSO_4$, and evaporated to dryness under reduced pressure. Further purification was carried out by Soxhlet extraction with acetone for 72 h to obtain **F-sub-PC** as a dark purple solid (63.2 mg, 0.0191 mmol, 13% yield). NMR spectra could not be obtained due to low solubility and aggregation. **MALDI-TOF MS**: m/z calcd. for $C_{84}H_{30}BClF_{102}N_6S_6$ $[M]^+$: 3297.9009, found: 3297.8978. UV/Vis (HFE7500): λ_{max} (log ε) =359 (4.3), 592 (4.2).

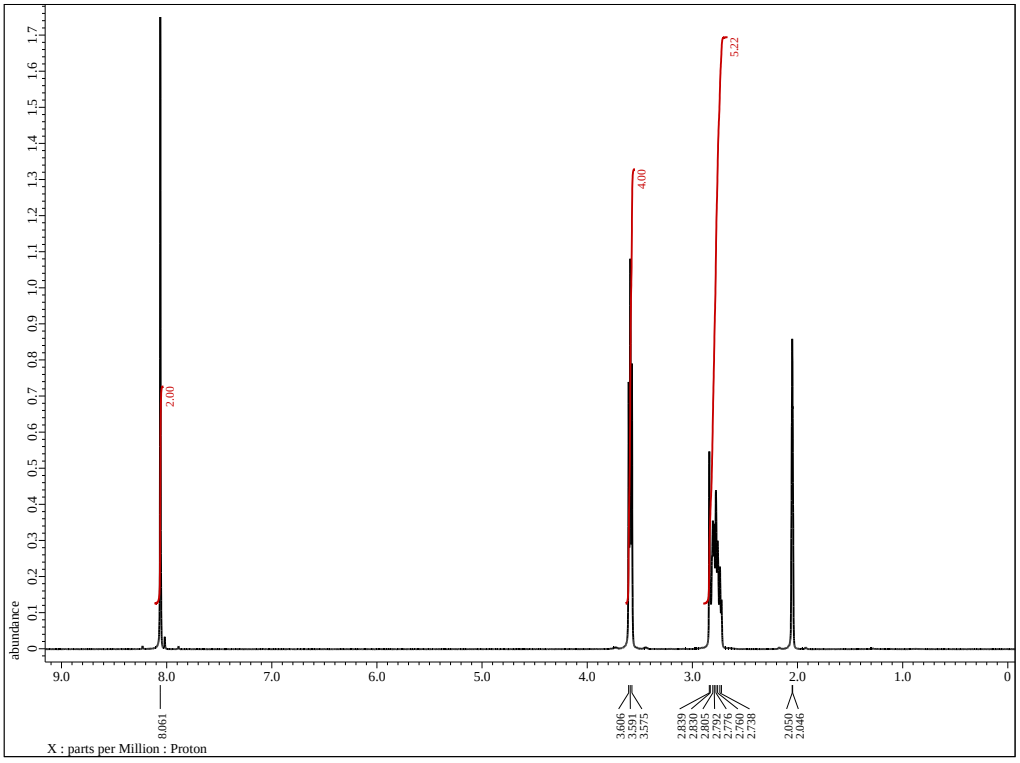

Figure S9. ^{1}H NMR (500 MHz, acetone-d_6, 25 °C) spectrum of Compound **3**.

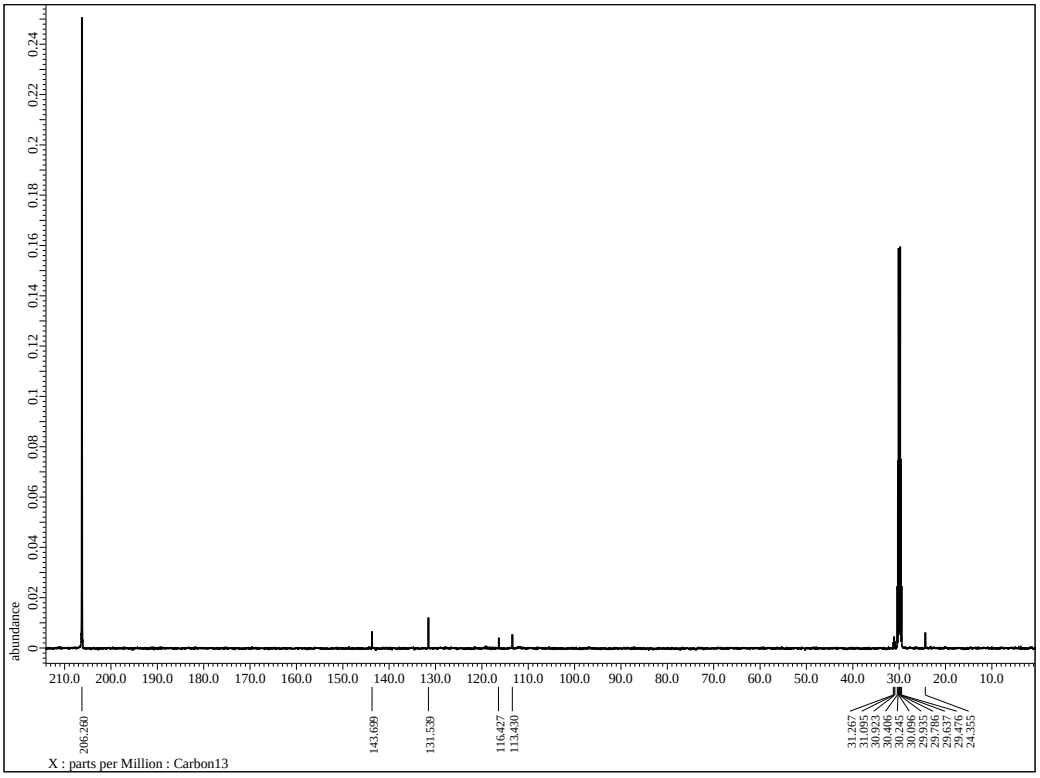

Figure S10. ^{13}C NMR (126 MHz, acetone-d_6, 25 °C) spectrum of Compound **3**.

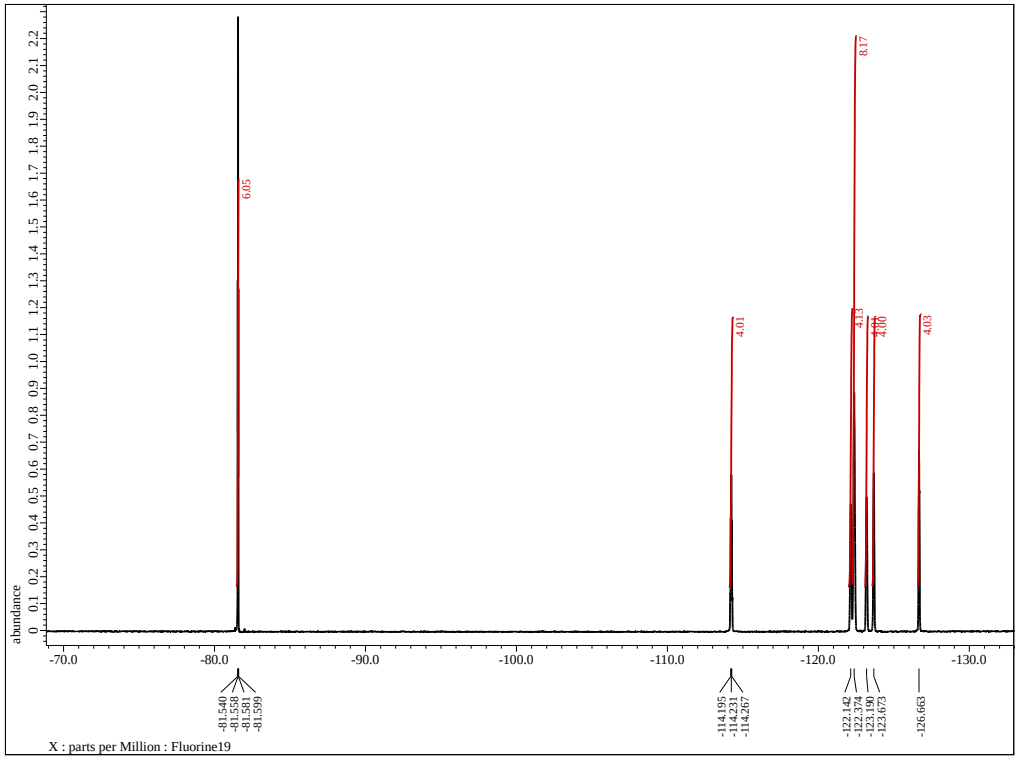

Figure S11. ^{19}F NMR (471 MHz, acetone-d_6, 25 °C) spectrum of Compound **3**.

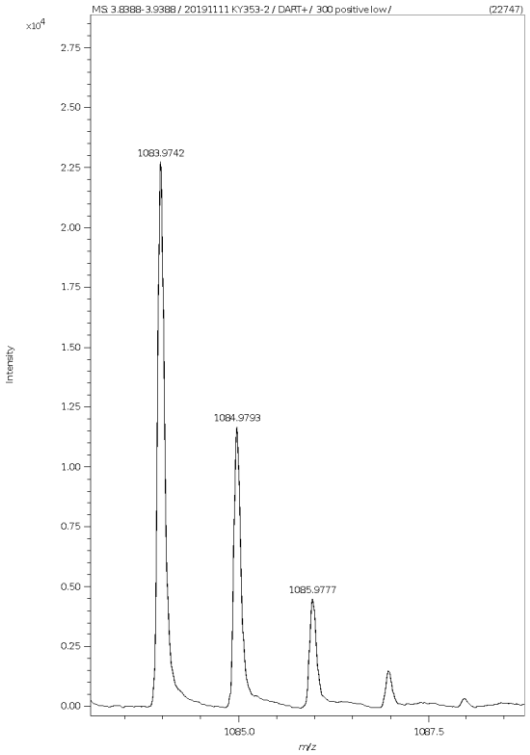

Figure S12. DART MS spectrum of Compound **3**.

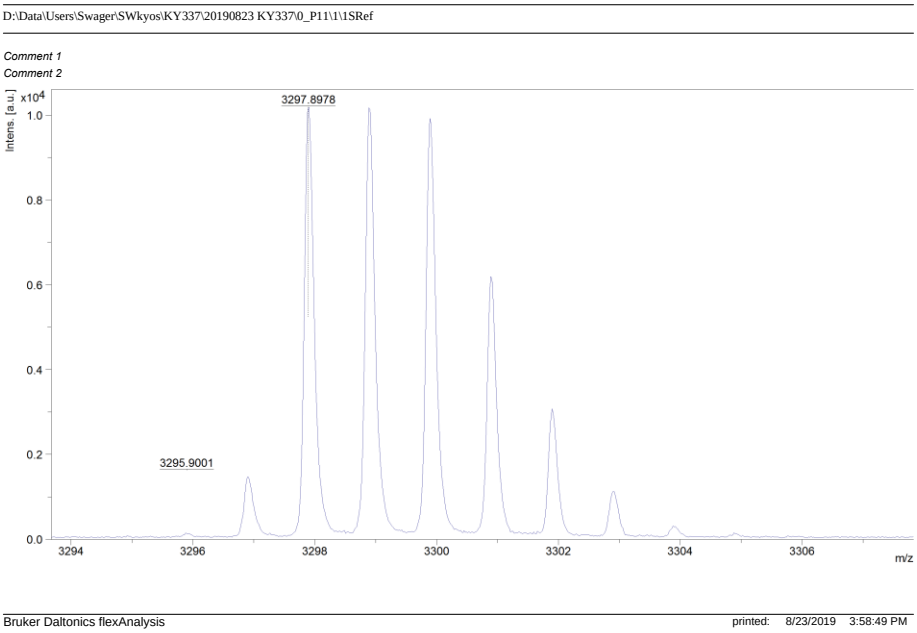

Figure S13. MALDI TOF-MS spectrum of **F-sub-PC**.

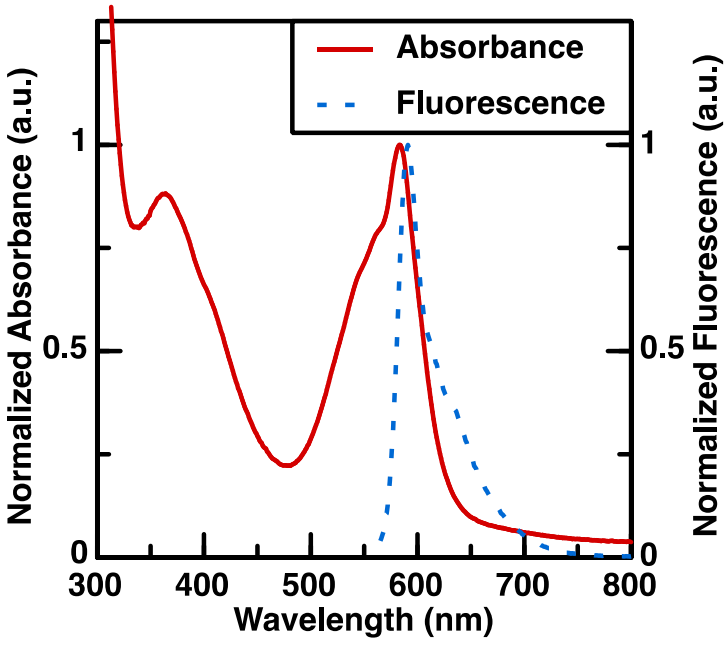

Figure S14. UV/Vis absorbance and fluorescence spectrum of **F-sub-PC** (solvent: HFE7500).

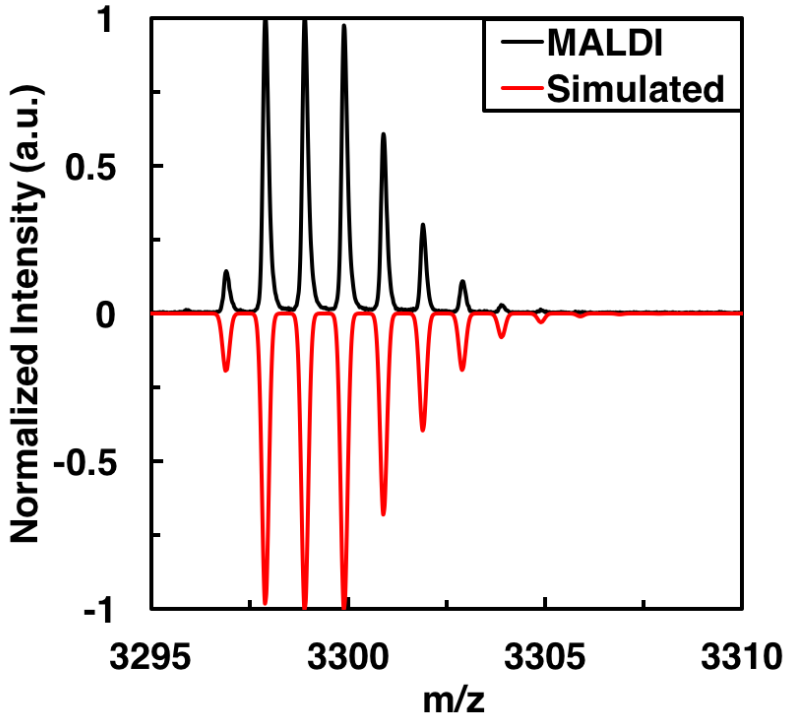

Figure S15. MALDI TOF-MS Isotope Distribution Comparison of **F-sub-PC**.

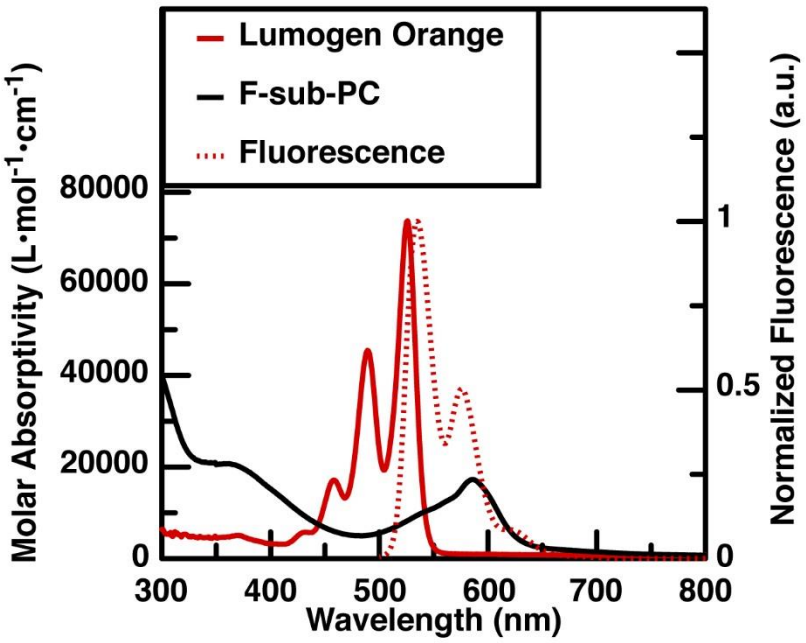

Figure S16. UV/Vis spectra of **F-sub-PC** in HFE7500 and **Lumogen F Orange 240** in diethylbenzene, overlayed with fluorescence specrum of **Lumogen F Orange 240** in diethylbenzene.

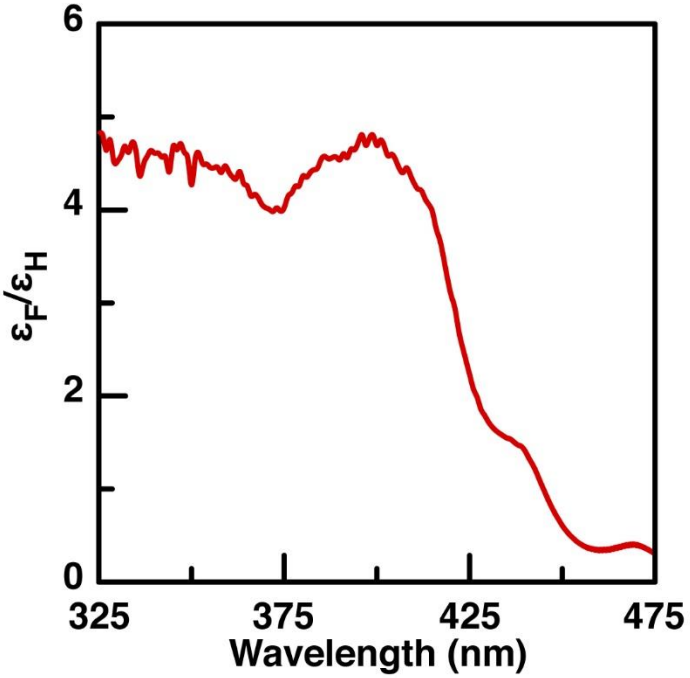

Figure S17. Ratio of molar absorptivity of **F-sub-PC** (ε_F) and **Lumogen F Orange 240** (ε_H).

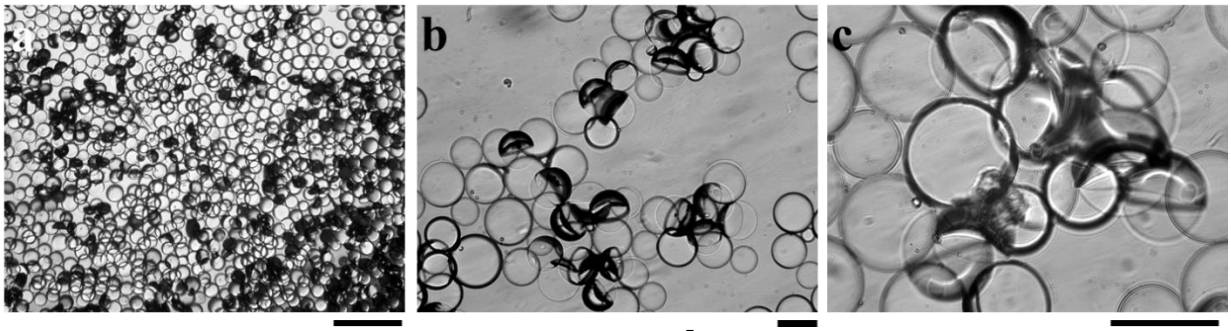

Figure S18. Optical images of droplets after adding 10^5 CFU/mL Listeria for 2h. Scale bar of a = 200 μm; scale bar of b,c = 50 μm.

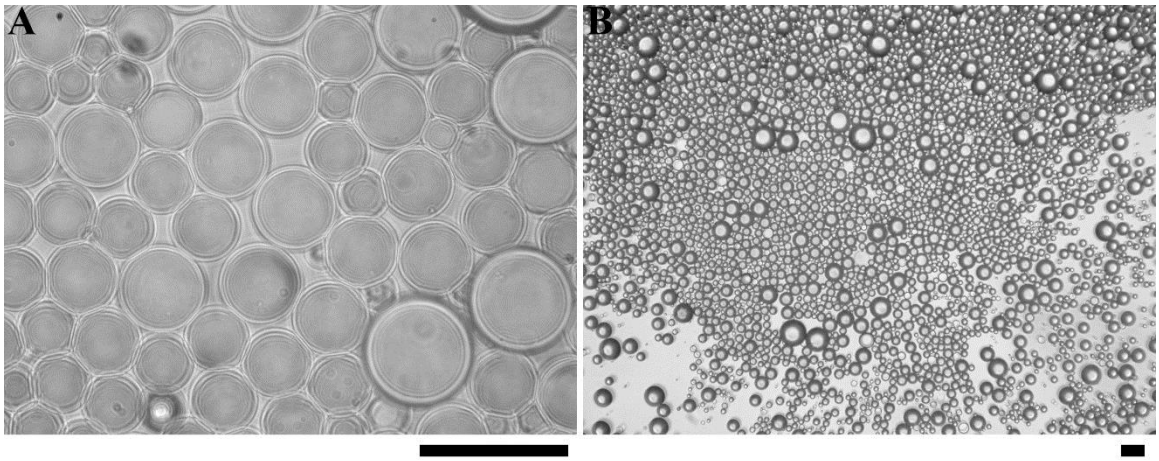

Figure S19. Optical images of Poly-TCO droplets after adding 10^7 CFU/mL of Bacillus subtilis for 2h (scale bar = 50 μm).

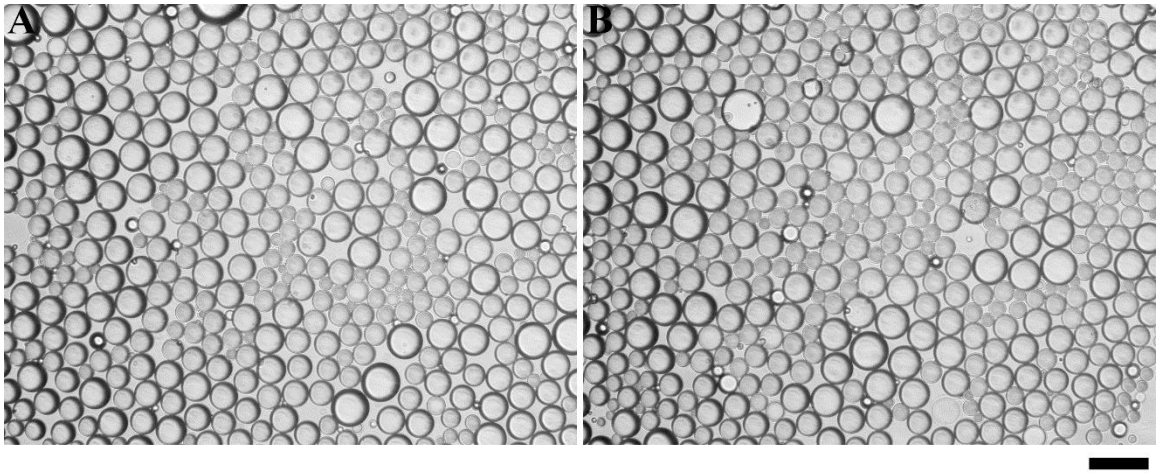

Figure S20. Optical images of Poly-TCO droplets after adding (A)10^7 CFU/mL of heat killed Salmonella; (B) Bovine serum albumin for 2h (scale bar = 50 μm).

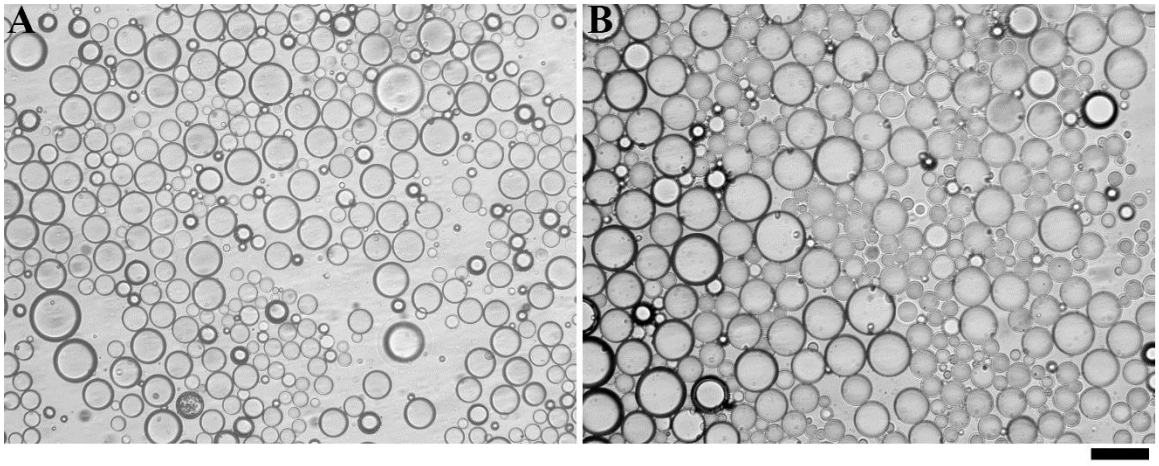

Figure S21. Optical images of (A) droplets prepared in synthetic blood; (B) droplets prepared in serum (scale bar = 50 μm).

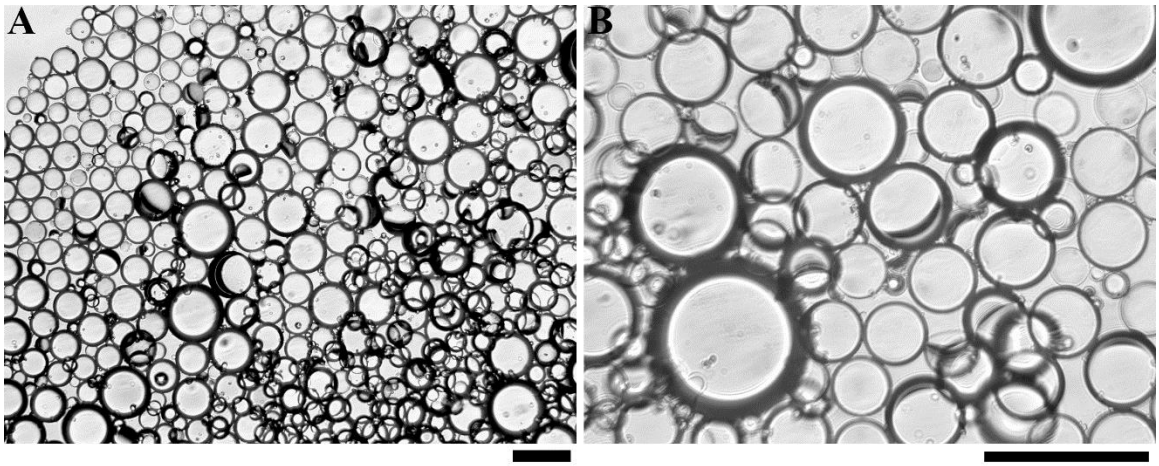

Figure S22. Optical images of droplets bioconjugated with Listeria antibody and then incubated with 10^7 CFU/mL of Listeria for 2h in serum (scale bar = 50 μm).

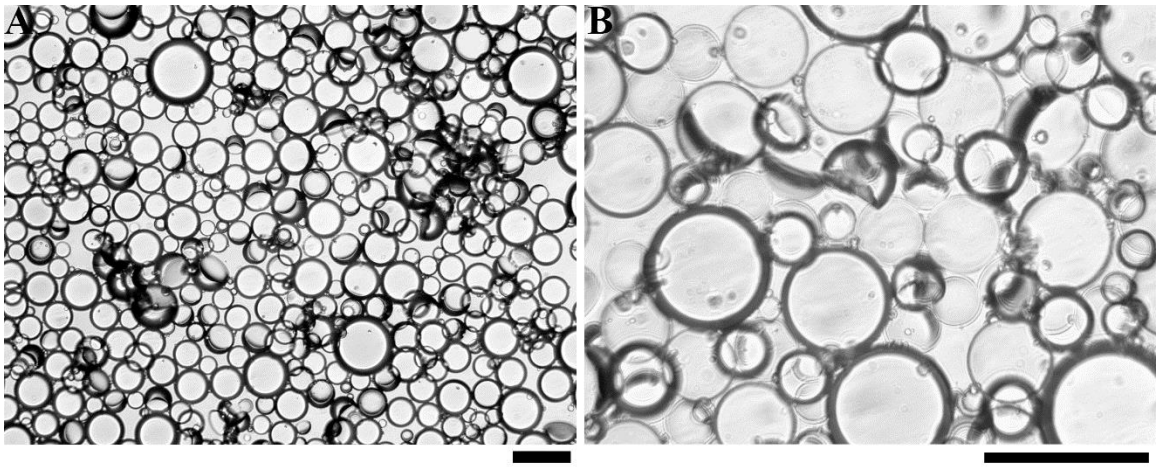

Figure S23. Optical images of droplets bioconjugated with Listeria antibody and then incubated with 10^7 CFU/mL of Listeria for 2h in synthetic blood (scale bar = 50 μm).

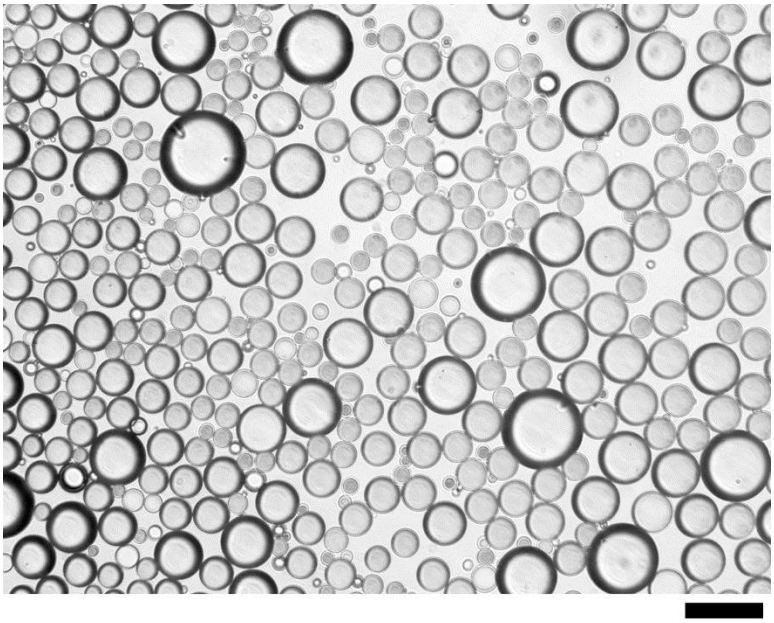

Figure S24. Optical images of droplets prepared in brain heart infusion broth (scale bar = 50 μm).

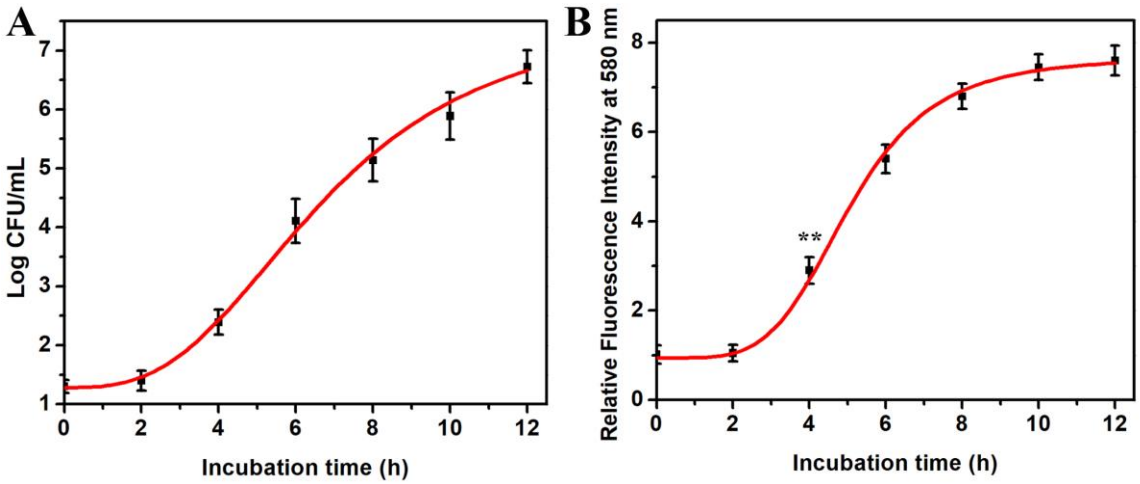

Figure S25. (A) Growth curves for Listeria monocytogenes in brain heart infusion broth at 20 CFU/mL and the cultures were incubated at 37°C in an incubator; (B) correlation of incubation time of Listeria (initial concentration at 20 CFU/mL) and relative fluorescence intensity (fluorescence spectra (λ_{ex}=361nm) of droplet containing Poly-TCO and sub-PC dye in the hydrocarbon phase, F-PBI dye in the fluorocarbon phase after addition of Listeria at different time points) at 580 nm (three replicate measurements were performed for the error bars, **p≤0.01).

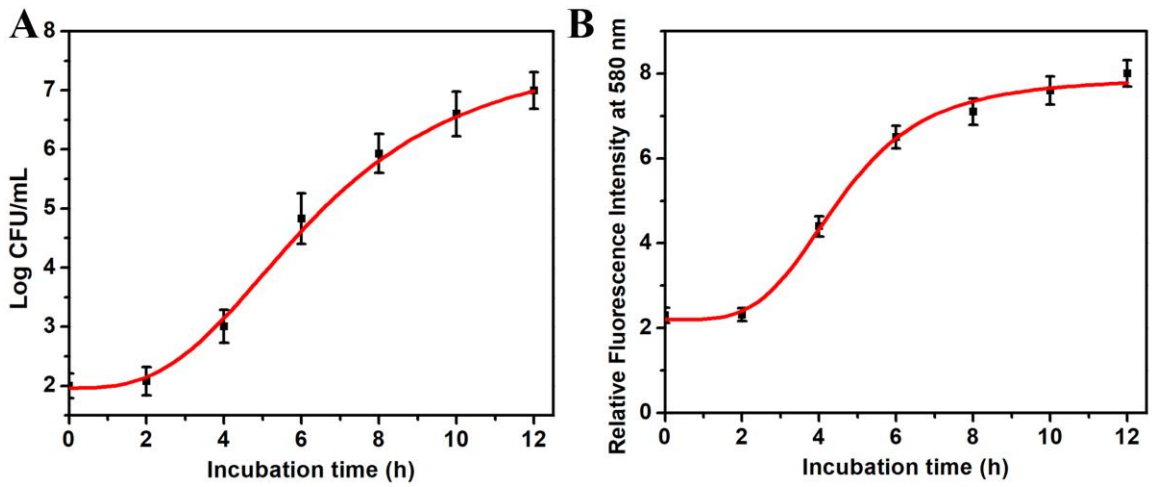

Figure S26. (A) Growth curves for Listeria monocytogenes in brain heart infusion broth at 100 CFU/mL and the cultures were incubated at 37°C in an incubator; (B) correlation of incubation time of Listeria (initial concentration at 100 CFU/mL) and relative fluorescence intensity (fluorescence spectra (λ_{ex}=361nm) of droplet containing Poly-TCO and sub-PC dye in the hydrocarbon phase, F-PBI dye in the fluorocarbon phase after addition of Listeria at different time points) at 580 nm (three replicate measurements were performed for the error bars).

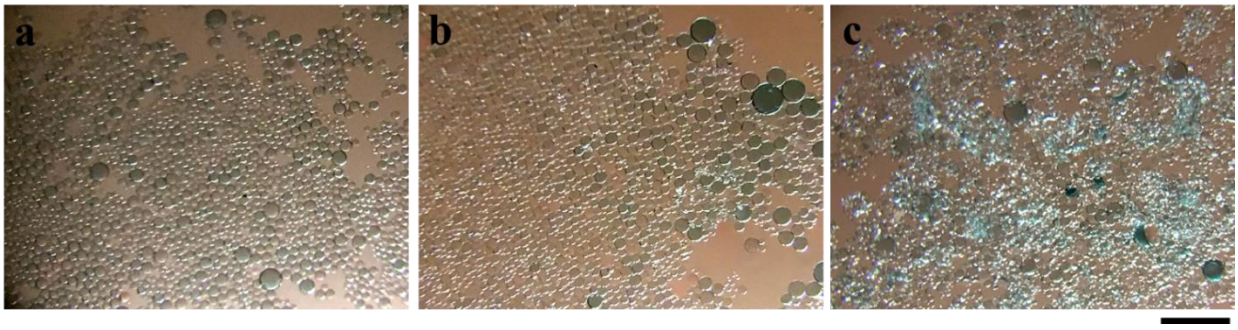

Figure S27. Optical images taken by smartphone of (a) non-agglutinated droplet (without addition of Listeria); (b) agglutinated droplets (with the addition of Listeria at 10^2 CFU/mL); (c) agglutinated droplets (with the addition of Listeria at 10^7 CFU/mL); with sub-PC dye (subphthalocyanine) in the hydrocarbon phase and F-PBI dye in the fluorocarbon phase. Scale bar= 200 μm.

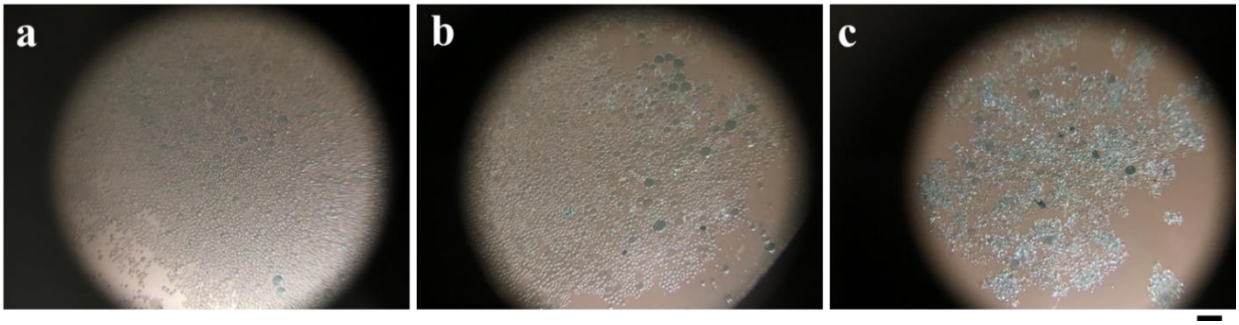

Figure S28. Optical images taken by smartphone of (a) non-agglutinated droplet (without addition of Listeria); (b) agglutinated droplets (with the addition of Listeria at 10^2 CFU/mL); (c) agglutinated droplets (with the addition of Listeria at 10^7 CFU/mL); with sub-PC dye (subphthalocyanine) in the hydrocarbon phase and F-PBI dye in the fluorocarbon phase. Scale bar= 200 μm.

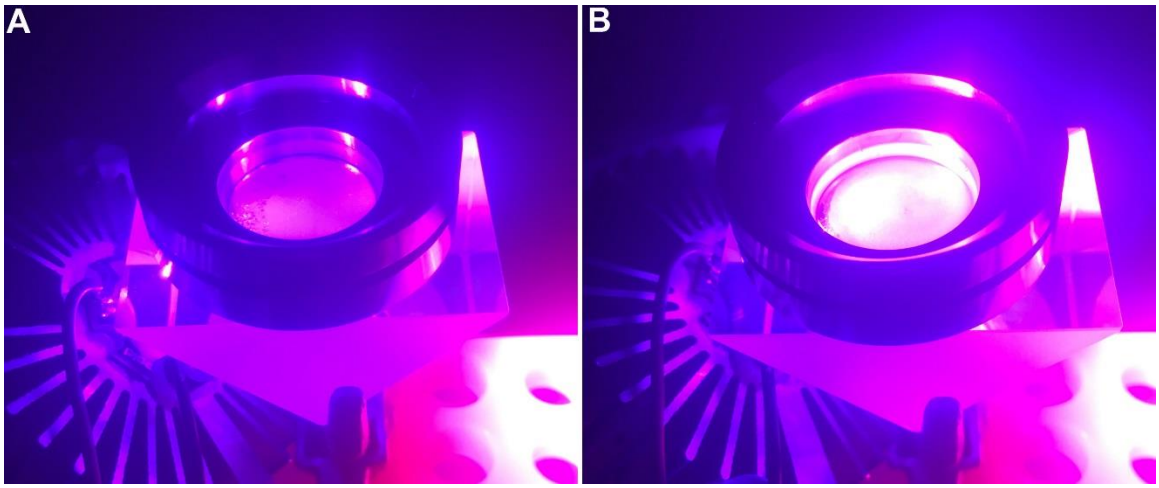

Figure S29. Images of Janus droplets on top of the waveguide device taken (A) without; (B) with the addition of Listeria.

References

1. Ong, W. J.; Swager, T. M. *Nature Chemistry* **2018**, *10*, 1023-1030
2. Claessens, C. G.; González-Rodríguez, D.; Del Rey, B.; Torres, T.; Mark, G.; Schuchmann, H. P.; Von Sonntag, C.; MacDonald, J. G.; Nohr, R. S. *European J. Org. Chem.* **2003**, *14*, 2547.